the FEBS Journal

PP3 forms stable tetrameric structures through hydrophobic interactions via the C-terminal amphipathic helix and undergoes reversible thermal dissociation and denaturation

Lise R. L. Pedersen[1,2], Søren B. Nielsen[2,3,4], Jon G. Hansted[2,3,4], Torben E. Petersen[1], Daniel E. Otzen[2,3,4,*] and Esben S. Sørensen[1,2,*]

1 Protein Chemistry Laboratory, Department of Molecular Biology and Genetics, Aarhus University, Denmark
2 Interdisciplinary Nanoscience Center (iNANO), Aarhus University, Denmark
3 Protein Biophysics Group, Department of Molecular Biology and Genetics, Aarhus University, Denmark
4 Center for Insoluble Protein Structures (inSPIN), Aarhus University, Denmark

Keywords
asymmetric flow field-flow fractionation; bovine milk; lactophorin; multimerization; proteose peptone component 3

Correspondence
E. S. Sørensen, Department of Molecular Biology and Genetics, Aarhus University, Science Park Aarhus, Gustav Wieds Vej 10 C, DK-8000 C Aarhus, Denmark
Fax: +45 89425044
Tel: +45 89425092
E-mail: ess@mb.au.dk
D. E. Otzen, Interdisciplinary Nanoscience Center (iNANO), Department of Molecular Biology and Genetics, Aarhus University, Science Park Aarhus, Gustav Wieds Vej 10 C, DK-8000 C Aarhus, Denmark
Fax: +45 86123178
Tel: +45 89425046
E-mail: dao@inano.dk

*These authors contributed equally to this work

(Received 31 August 2011, revised 14 November 2011, accepted 15 November 2011)

doi:10.1111/j.1742-4658.2011.08428.x

The milk protein proteose peptone component 3 (PP3), also called lactophorin, is a small phosphoglycoprotein that is expressed exclusively in lactating mammary tissue. The C-terminal part of the protein contains an amphipathic helix, which, upon proteolytic liberation, shows antibacterial activity. Previous studies indicate that PP3 forms multimeric structures and inhibits lipolysis in milk. PP3 is the principal component of the proteose peptone fraction of milk. This fraction is obtained by heating and acidifying skimmed milk, and in the dairy industry milk products are also typically exposed to treatments such as pasteurization, which potentially could result in irreversible denaturation and inactivation of bioactive components. We show here, by the use of CD, that PP3 undergoes reversible thermal denaturation and that the α-helical structure of PP3 remains stable even at gastric pH levels. This suggests that the secondary structure survives treatment during the purification and possibly some of the industrial processing of milk. Finally, asymmetric flow field-flow fractionation and multi-angle light scattering reveal that PP3 forms a rather stable tetrameric complex, which dissociates and unfolds in guanidinium chloride. The cooperative unfolding of PP3 was completely removed by the surfactant *n*-dodecyl-β-D-maltoside and by oleic acid. We interpret this to mean that the PP3 monomers associate through hydrophobic interactions via the hydrophobic surface of the amphipathic helix. These observations suggest that PP3 tetramers act as reservoirs of PP3 molecules, which in the monomeric state may stabilize the milk fat globule.

Structured digital abstract

- PP3 and PP3 bind by circular dichroism (View interaction)
- PP3 and PP3 bind by molecular sieving (View interaction)
- PP3 and PP3 bind by fluorescence technology (View interaction)
- PP3 and PP3 bind by molecular sieving (View interaction)

Abbreviations
AF4, asymmetric flow field-flow fractionation; DDM, *n*-dodecyl-β-D-maltoside; DOPC, 1,2-dioleoylphosphatidylcholine; DOPG, 1,2-dioleoylphosphatidylglycerol; GdmCl, guanidinium chloride; MALS, multi-angle light scattering; MRE, mean residue ellipticity; OA, oleic acid; PP3, proteose peptone component 3; RI, refractive index; SEC, size exclusion chromatography; TFE, trifluoroethanol.

Introduction

Heating of skimmed milk (95 °C, 30 min) followed by acidification to pH 4.6 causes the denaturation of most whey proteins and their co-precipitation with caseins, leaving a heterogeneous protein fraction in solution. This fraction is designated the proteose peptone [1,2]. The proteose peptone fraction of bovine milk is a complex mixture of glycoproteins, phosphoproteins and peptides, contributing approximately 1 g of protein per litre of skimmed milk [3]. The main constituents of the fraction are fragments and phosphopeptides derived from plasmin digestion of caseins [4]. However, the fraction also comprises highly soluble proteins not related to caseins.

The principal component of the fraction is a small phosphoglycoprotein designated proteose peptone component 3 (PP3) [5] or lactophorin [6,7]. PP3 constitutes approximately 25% of the proteose peptone fraction, amounting to 200–300 $mg \cdot L^{-1}$ of skimmed milk [8]. PP3 is not expressed in humans, but it has been characterized in the milk of several species of ruminants, where it is exclusively expressed in the lactating mammary tissue [9–15]. However, a homologous protein called glycosylation-dependent adhesion molecule (GlyCAM-1), which shows 56% similarity to the bovine protein, has been found in several tissues in mice and rats [16–21] as well as in the ovine uterus [22].

Bovine PP3 protein consists of 135 amino acids and contains five phosphoserines, three O-glycosylations and one N-glycosylation, giving a total molecular mass of 19.3 kDa [23,24]. PP3 is a substrate for plasmin in milk, and a proteolytic fragment corresponding to residues 54–135 has been found to be associated with full-length PP3 protein in milk. In SDS/PAGE, PP3 and the naturally occurring proteolytic fragment (residues 54–135) migrate at positions equivalent to a molecular mass of approximately 28 and 17 kDa, respectively [15]. This anomalous migration can probably be explained by the highly acidic nature of the components and hence poor pairing with the SDS. Interestingly, NMR studies show that a peptide modelled from the C-terminal residues 98–135 of PP3 forms a perfectly amphipathic membrane-binding α-helix that is oriented in plane with the membrane surface [25].

The function of PP3 *in vivo* is not clear. PP3 and derived fragments have shown immune-stimulating properties [26,27] and the ability to counteract acid attack on tooth mineral [28]. A larger fragment of PP3 was observed to act as a potent inhibitor of human rotavirus infections in embryonic monkey kidney cells and suckling mice [29]. A peptide (called lactophoricin), encompassing residues 113–135 of the C-terminal amphipathic helix of PP3, has been found to form pores in planar lipid bilayers as well as to display antibacterial activity against both Gram-positive and Gram-negative strains of bacteria [30–32]. PP3 has shown high affinity for oil surfaces and the ability to stabilize emulsified oil globules in emulsions; hence, the protein is a strong emulsifying and foaming agent [33]. The affinity for lipids has led to the hypothesis that PP3 could act as a natural inhibitor of spontaneous lipolysis in milk by binding to the milk fat globule membrane [34].

In several studies, PP3 has been observed to form what appears to be homomultimers in bovine milk [11,35,36]. This aggregation or multimerization has been suggested to be mediated by interaction between the hydrophobic parts of the C-terminal amphipathic α-helices [25,37]. This formation of multimers could potentially be important in the interaction of PP3 with lipids, as well as in the interaction of PP3-derived peptides with membranes.

Besides the high temperatures and acidic environment to which the milk protein is subjected during isolation in the laboratory, milk and other dairy products are normally exposed to high temperatures during pasteurization processes to increase shelf life and to kill potential health-compromising microorganisms. However, this process also denatures many milk proteins with potential beneficial properties, so-called bioactive milk proteins [38].

Here we have examined the structural stability and multimeric nature of PP3 by CD to analyze changes in secondary structure as a function of variation in pH and temperature. The molecular mass and sizes of PP3 aggregates or multimers were estimated by size-exclusion chromatography (SEC) and asymmetric flow field-flow fractionation (AF4). In summary, PP3 retains its α-helical structure between pH 2 and pH 9.2 and almost completely refolds to its native conformation upon thermal denaturation. Furthermore, PP3 was found to form higher-order structures, probably tetramers, which disassembled upon heating and in the presence of guanidinium chloride (GdmCl), non-denaturing surfactant micelles or the monounsaturated oleic acid (OA). This suggests that the tetramer structure is a storage state that provides a reservoir of PP3 molecules, which, in the monomeric state, may stabilize fat globules or serve as precursors for the proteolytic generation of bactericidal C-terminal peptides.

Results and Discussion

PP3 refolds upon thermal denaturation and the α-helical structure is stable at gastric pH values

Far-UV CD spectra of PP3 were recorded under physiological conditions as well as in the presence of anionic and other organic solvents known to stabilize α-helical structure. In all CD spectra, minima at 208 and 222 nm were observed (Fig. 1A), which indicate α-helical structure. Dissolving PP3 in micellar concentrations of SDS (1%; ~ 35 mM) led to a general increase in the CD signal and thus in the degree of α-helicity. This is consistent with the ability of micellar SDS to induce α-helical structure [39]. The greatest signal increase was obtained using 90% trifluoroethanol (TFE), which is known to stabilize helical conformation as a result of its hydrophilicity and hydrogen-bonding ability [40]. Neither 100% 1,2-dioleoylphosphatidylcholine (DOPC) vesicles nor 1,2-dioleoylphosphatidylcholine/1,2-dioleoylphosphatidylglycerol (DOPC/DOPG) vesicles, at a ratio of 80 : 20 (w/w), induced any spectral changes, indicating that phospholipid vesicles do not promote further formation of α-helical structure.

For isolation of the proteose peptone fraction containing PP3, high temperatures are used to precipitate the major whey proteins α-lactalbumin and β-lactoglobulin followed by acidification to pH 4.6 to precipitate the caseins [15]. CD wavelength scans of PP3 in aqueous buffer with pH values between 2 and 9.2 show that the α-helical structure is very stable throughout the tested pH range (Fig. 1B). To obtain complementary information on the tertiary structure, we turned to fluorescence. PP3 contains no tryptophan residues, but fluorescence emission spectra from the single tyrosine residue (at position 121) of PP3, acquired between pH 3 and pH 11, indicate no shift in the emission peak position and only small changes in fluorescence intensity. This indicates that the tertiary structure is essentially invariant and this is consistent with the lack of change in CD spectra (Fig. 1C). The studies of the biological functionalities of PP3 mainly focus on the C-terminal part of PP3, which contains the α-helical structure. These observations indicate that this structure is preserved during the elevated temperatures used in the purification of the protein [15] as well as in the acidic conditions encountered by the protein in the gastric juice.

CD was used to study the conformational changes that PP3 undergoes at higher temperatures and the extent of its reversibility. Spectra recorded at different temperatures during the scan (Fig. 2A) revealed two isodichroic points at ~ 205 and ~ 235 nm, indicating

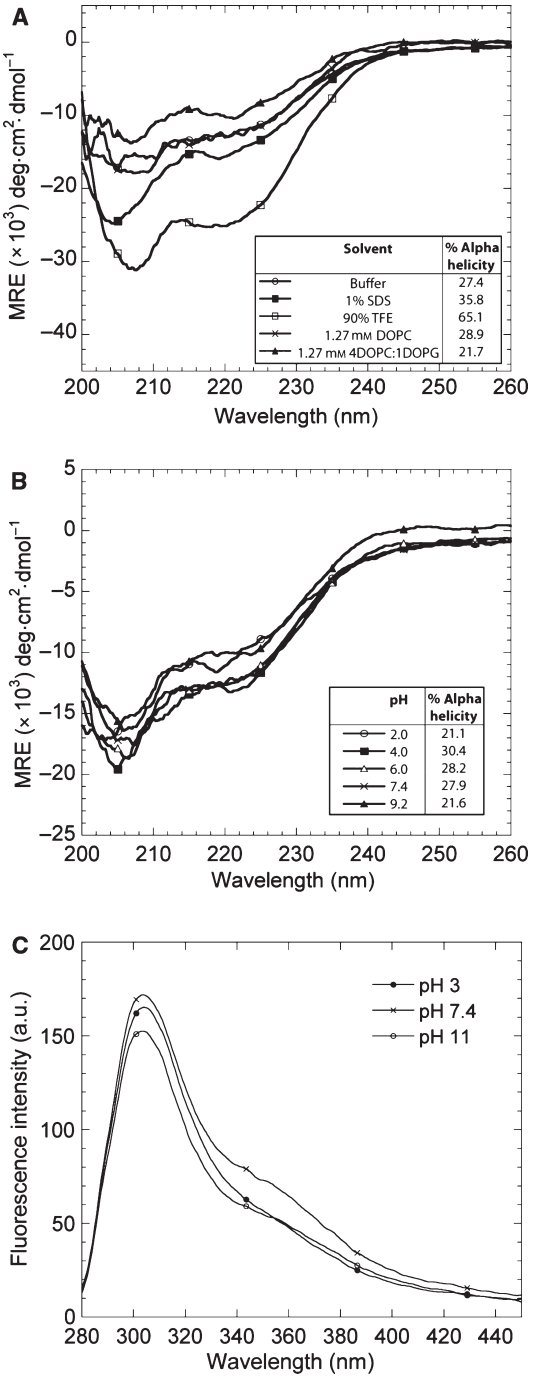

Fig. 1. The degree of α-helicity of PP3 increases in the presence of anionic and organic solvents and the α-helical structure is essentially invariant over the pH range 2.0–9.7. (A) CD wavelength spectra of 2.1 μM PP3 in mixtures of 10 mM Na_2HPO_4 (pH 7.4) (denoted buffer), 1% SDS, 90% TFE, 1.27 mM corresponding to 1 mg mL^{-1} of DOPC or 1.27 mM corresponding to 1 mg mL^{-1} of DOPC/DOPG at a ratio of 80 : 20 (w/w), at 25 °C. (B) CD wavelength spectra of 2.1 μM PP3 in 10 mM Na_2HPO_4 at pH values ranging from 2 to 9.2. Percentage α-helicity is given in the insert. (C) Steady-state tyrosine fluorescence of the tertiary structure of PP3 at pH 3, pH 7.4 and pH 11.

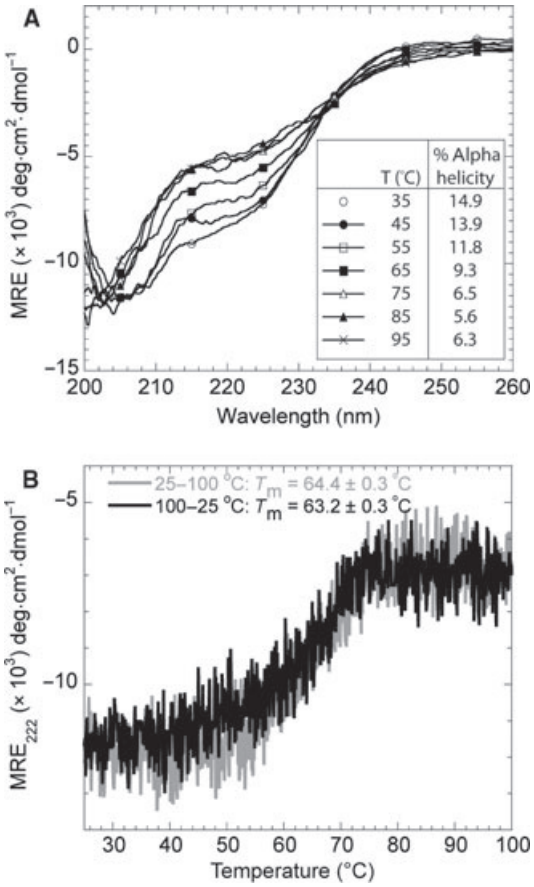

Fig. 2. PP3 refolds almost completely upon thermal denaturation. (A) CD wavelength spectra of 2.0 μM PP3 recorded at different temperatures. Percentage α-helicity is given in the insert. T, temperature. (B) Far-UV CD spectra of a forward (25 → 100 °C) and a backward (100 → 25 °C) thermal scan of 2.1 μM PP3 at 222 nm. The melting temperature (T_m) is indicated for each curve.

a simple two-state transition from the folded α-helical state to the unfolded random coil state. Forward (25 → 100 °C) and backward (100 → 25 °C) thermal scans indicated that most of the PP3 population was able to refold into the original conformation, as the backward scan led to a reduction of only 4.3% in ellipticity (Fig. 2B). Furthermore, the apparent melting temperature was only reduced from 64.4 ± 0.3 °C (forward scan) to 63.2 ± 0.3 °C (backward scan) (Fig. 2B). CD wavelength scans of the sample were performed at 25 °C immediately before and after the thermal scans and showed no conformational change, confirming that PP3 essentially refolds completely upon thermal denaturation (data not shown). These results indicate that the α-helical structure of PP3, and thereby the claimed positive effects conveyed by PP3 in milk, are preserved during industrial processing.

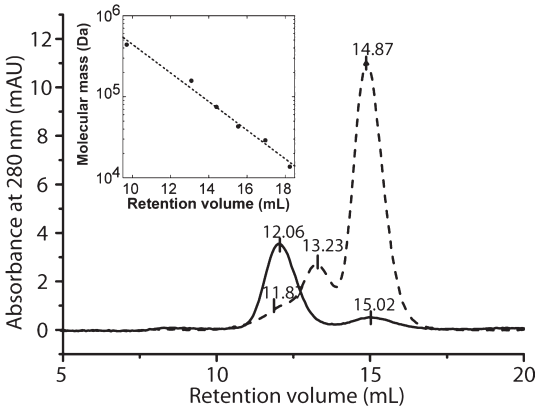

Fig. 3. The elution profile of PP3 subjected to SEC indicates aggregation of PP3 to form higher-order structures. Elution profiles of PP3 (solid line) and BSA (dashed line) were obtained by gel-filtration chromatography on a Superdex 200 column eluted with phosphate-buffered saline (NaCl/P_i), pH 7.5, at a flow rate of 0.8 mL·min^{-1}. A relative calibration with retention volumes of a set of standard proteins (14–440 kDa) is shown in the insert.

PP3 forms stable tetramers

To thoroughly analyze the multimerization or aggregation of PP3 observed in previous studies we used SEC and AF4 combined with multi-angle light scattering (MALS). Monomeric glycosylated PP3 has a molecular mass of 19.4 kDa [24]; however, SEC analysis of PP3 showed a major peak eluting at 12.06 mL, corresponding to a relative molecular mass of ~ 191 kDa. A smaller peak eluted at 15.02 mL, corresponding to a molecular mass of ~ 58 kDa (Fig. 3). This indicates that PP3 preferentially assembles into multimeric structures under these conditions. These results are in agreement with previous SEC measurements of the PP3 multimers, where PP3 eluted at an elution volume corresponding to a molecular mass of approximately 190 kDa [11]. Analyses of PP3 by AF4 showed similar results, with relative molecular mass estimates of 225.9 kDa for the high-molecular-mass peak and 23.4 kDa for the low-molecular-mass peak (Fig. 4A).

Using AF4/MALS, the molecular mass can be determined independently from light scattering data by extrapolation to a zero sample concentration and a zero scattering angle using the Zimm model. This MALS-based analysis requires the sample concentration to be determined either by the refractive index (RI) (based on both protein and carbohydrate contributions, see the Materials and methods) or by the absorbance at 205 nm (giving only protein contributions). In separate experiments exemplified in Fig. 4B, the molecular mass of the main PP3 peak was determined

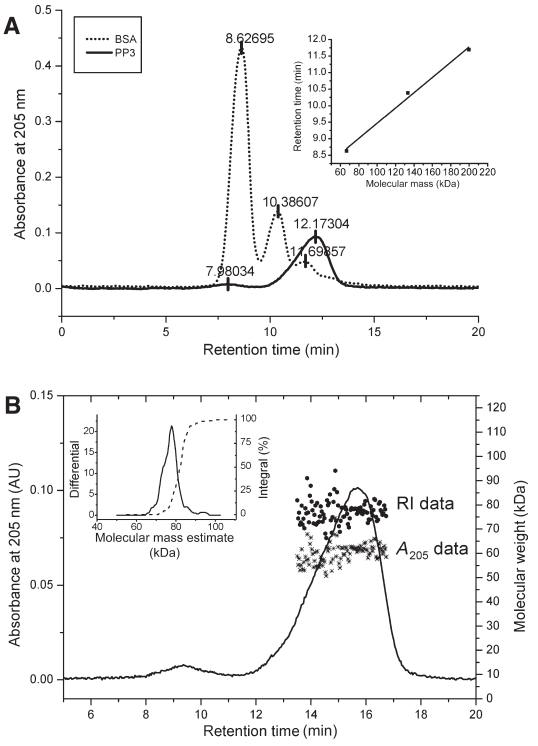

Fig. 4. PP3 monomers associate into highly extended and stable tetrameric complexes. (A) Elution profile of PP3 (solid line) and BSA (dashed line) upon separation by AF4, monitored by UV light (A_{205}). The insert shows the relative calibration in which the retention time of BSA monomers, dimers and trimers was plotted as a function of molecular mass. (B) AF4/MALS estimates of the molecular mass of PP3 multimers using RI (●) and A_{205} nm (✳) data to obtain size estimates of PP3 with and without glycosylation, respectively. The insert shows the distribution of PP3 multimer size estimates. The mobile phase consists of 5 mM Tris/HCl containing 150 mM NaCl.

in combination with RI data to be 79.1 ± 2.6 kDa (mean ± standard error of three individual analyses) using the weight-averaged $(dn/dc)_{PP3}$. This value corresponds to approximately four PP3 units of ~ 19.8 ± 0.7 kDa protein assembled into a tetrameric complex. The molecular mass of post-translationally modified PP3 has previously been determined, by mass spectrometric analysis, to be 19.4 ± 0.02 kDa [24], which is in excellent agreement with the present results. Using MALS combined with absorbance data at 205 nm (which lacks carbohydrate contributions), the main peak was determined to be 61.1 ± 1.5 kDa, corresponding to four, 15.3 ± 0.4-kDa units and thus within ~ 3% of the theoretical molecular mass of the PP3 polypeptide chain. The difference of ~ 4.5 kDa between monomer size estimates thus arises as a result of the inability to detect glycosylations and phosphorylations by measuring the absorbance at 205 nm. In fact, the molecular mass of the post-translational modifications of PP3 has previously been determined to constitute 4.1 ± 0.02 kDa [24]. The validity of size estimates were further confirmed by size estimation of BSA monomers and dimers using a $(dn/dc)_{BSA}$ of 0.186 $mL \cdot g^{-1}$ [41,42] in a separate AF4/MALS experiment, which revealed molecular mass values of 64.5 and 135 kDa, respectively.

In AF4/MALS, sample retention relies on the diffusion coefficient (which can be related to the radius for strictly spherical particles through the Stokes–Einstein equation) and liquid flows inside the separation channel. Unfortunately, the 635-nm laser of our MALS limits reliable size estimates to > 32 nm (limit = $\lambda/20$) and thus does not allow reliable estimates of BSA and PP3 sizes and hence the evaluation of protein compactness. However, the molecular mass estimates of MALS, in combination with the high retention times (indicating a large hydrodynamic size compared with BSA) of PP3 in AF4/MALS separation, clearly suggest that PP3 preferentially assembles into a highly extended tetrameric complex of ~ 79 kDa. We further analyzed the monomer/tetramer distribution as a function of protein concentration by AF4 and found a constant ratio of ~ 3.8 ± 0.2% monomer and 96.2 ± 0.2% tetramer at six concentrations between 0.93 $mg \cdot mL^{-1}$ (~ 50 μM) and 7.72 $mg \cdot mL^{-1}$ (~ 415 μM) PP3 (data not shown), suggesting that the tetrameric complex is rather stable in the absence of denaturing agents.

To monitor the unfolding and potential dissociation of the tetramer during unfolding by GdmCl, steady-state fluorescence anisotropy and CD were used. As shown in Fig. 5, the anisotropy decreases above ~ 1 M GdmCl, clearly indicating that PP3 tumbles faster in solution under these conditions. While protein unfolding is expected to increase the hydrodynamic radius of the protein and thus decrease the tumbling rate (larger anisotropy), the decrease in anisotropy is consistent with dissociation of the tetrameric complex. Monitoring of the GdmCl-mediated unfolding of PP3 by CD further shows that the dissociation of the PP3 complex is accompanied by loss of α-helix structure measured at 220 nm and thus the PP3 complex dissociates as a result of chemical denaturation (Fig. 5). The fluorescence anisotropy and the CD recordings at 50 μM PP3 show transitions with midpoints at 2.10 ± 0.06 M GdmCl and 50% unfolding at 2.16 ± 0.04 M GdmCl, respectively. These values are equal within error and thus indicate that tetramer dissociation and loss of helical structure occur in parallel.

To investigate the effect of milk fat globules or globule mimics on this structure, a simple separation-free

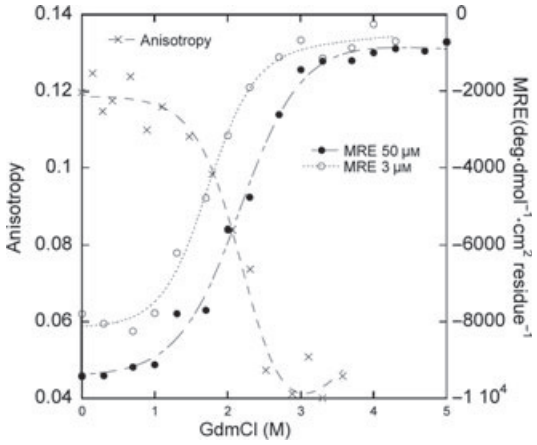

Fig. 5. PP3 multimers dissociate and monomers unfold in the presence of GdmCl. The steady-state tyrosine fluoroscence anisotropy and mean residue ellipticity (MRE) of PP3 at 220 nm were plotted as a function of GdmCl concentration. MRE data were recorded at both 3 and 50 μM (the anisotropy signal was too weak to be recorded at 3 μM). Data were fitted to Eqn (3).

assay was developed to monitor loss of higher-order structure. If the loss of structure occurring during thermal-reversible denaturation is coupled to higher-order structure, it will be concentration dependent and thermal stability will increase with PP3 concentration. Indeed, over the PP3 concentration range of 2.1–30 μM, unfolding remained cooperative while the melting temperature increased with PP3 concentration (Fig. 6A). Consistently, unfolding transitions in GdmCl monitored by far-UV CD showed a midpoint shift from 1.75 ± 0.05 M at 3 μM to 2.16 ± 0.04 M at 50 μM (Fig. 5) (the anisotropy signal at 3 μM was too weak to allow us to follow tetramer dissociation at this concentration). These sets of data show that stability increases with protein concentration (i.e. unfolding is associated with dissociation). CD wavescans of PP3 over the range 2.1–30 μM showed essentially no difference in the CD spectra (Fig. 6B). This observation, supported by the constant ratio between monomeric and tetrameric PP3 in the AF4 chromatograms over a wide concentration range (see above), revealed that the PP3 tetramer is relatively stable in the absence of denaturing agents.

Using this assay, we investigated whether the higher-order structure could be disrupted by external agents mimicking milk fat globules. As mimics we chose a nonionic surfactant, *n*-dodecyl-β-D-maltoside (DDM), and the unsaturated fatty acid, OA. DDM and OA were used at 1 mM and at 3.5 mM, respectively, which are well above their critical micelle concentrations of 0.17 and 0.006 mM, respectively. Both mimics completely removed the cooperative unfolding signal of 2 μM PP3 (Fig. 6C,D), strongly suggesting that the protein had lost its ability to undergo cooperative unfolding. Generally, nonionic surfactants, such as DDM, do not bind and destabilize individual protein molecules [39], although there are exceptions for

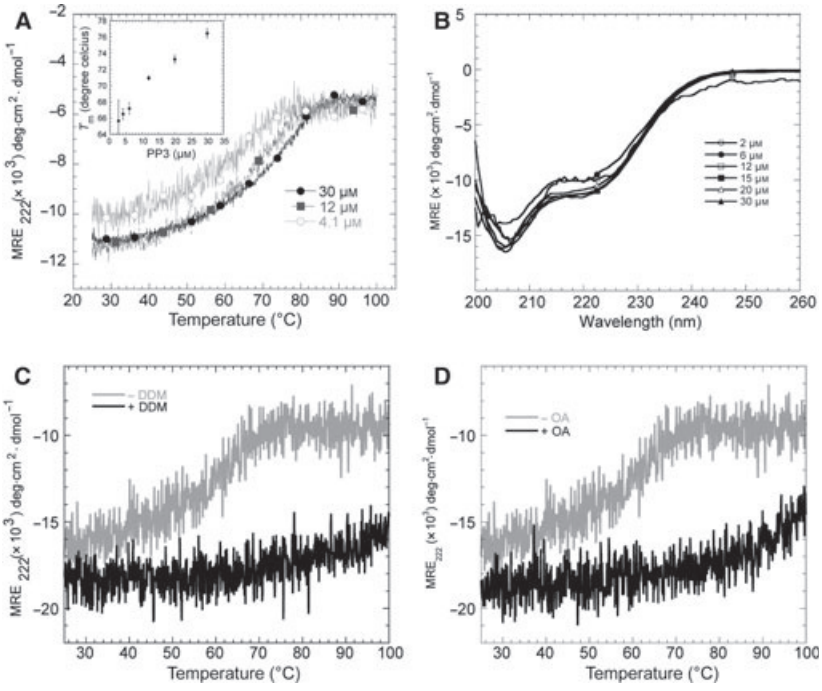

Fig. 6. Loss of structure of PP3 during thermal denaturation is concentration dependent and indicates that PP3 monomers associate via hydrophobic interactions. (A) Representative thermal far-UV CD scans, at 222 nm, of 4.1, 12 and 30 μM PP3. Curves were fitted to Eqn (2), and melting temperatures with a fitting error are shown in the insert. (B) CD wavelength scans of PP3 concentration over the range 2.1–30 μM. (C) Thermal far-UV CD scan, at 222 nm, of 2 μM PP3, with or without 1 mM DDM, as a function of temperature. (D) Thermal far-UV CD scan, at 222 nm, of 2 μM PP3, with or without 3.5 mM OA, as a function of temperature.

proteins with hydrophobic binding sites, such as α-lactalbumin [43] and cutinase [44]. The loss of cooperative unfolding by DDM indicates that the surfactant perturbs the tetramer structure in some way. This could be either by partially disordering the tetramer so that the monomers are held together more loosely, or simply by dissociating the tetramer to individual components. It is very difficult to distinguish these options by conventional separation techniques because the DDM micelles, which have a range of sizes, will contribute to the molecular weight. Although we thus cannot rule out the 'loose tetramer' option, we favour the simpler model that PP3 monomers associate through hydrophobic interactions via the hydrophobic surface of the amphipathic helix (Fig. 7), and these interactions are disrupted by the alkyl chains of the nonionic surfactant. Given that OA (monounsaturated) is one of the most common fatty acids in milk [~ 0.8% (w/v) [45]], it could be speculated that the PP3 tetramers may exist as a reservoir that dissociates upon binding to milk fat globules.

In conclusion, the results presented in this paper suggest that bovine milk PP3 is able to refold to its native state after being exposed to extreme temperatures and pH conditions. Likewise, the studies indicate that the α-helical structure of PP3 withstands both the low pH present in the digestive system as well as the high temperatures used for pasteurization of milk products in the dairy industry. It is also shown that PP3 monomers associate into rather stable tetrameric complexes independent of protein concentration, and the results indicate that these monomers associate via hydrophobic interactions.

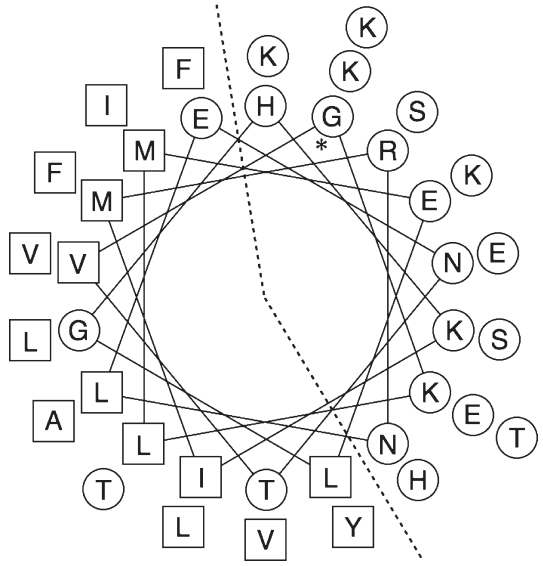

Fig. 7. The C-terminal helix of PP3 is amphipathic. Helical wheel plot of the C-terminal 38 residues of bovine PP3. Neutral and hydrophilic residues are within circles and hydrophobic residues are within squares. The asterisk (*) marks the N terminus of the peptide. The distinction between the primarily hydrophobic side and the hydrophilic side of the amphipathic helix is indicated by the dashed line.

As mentioned in the Introduction, PP3 or the homologue lactophorin has been isolated and characterized functionally from a number of species. Camel lactophorin, in particular, has been studied in detail. Camel lactophorin has high sequence identity with the bovine PP3 sequence, and the C-terminal sequence encoding the amphipathic α-helix in bovine PP3 is highly conserved in camel lactophorin [9,46,47]. The concentration of lactophorin in camel milk was about three times higher than the concentration of the homologue in bovine milk and has been suggested to function as an inhibitor of lipolysis, as described for bovine PP3 [46].

In bovine milk a significant fraction of the PP3 protein undergoes proteolytic digestion with the endogenous protease plasmin [15]. This results in the generation of a C-terminal peptide containing the amphipathic α-helix. Previously, a synthetic peptide, called lactophoricin, corresponding to this C-terminal part of PP3, was shown to possess antibacterial activity [31]. PP3 has also previously been shown to function as an inhibitor of lipolysis [48]. We therefore suggest the following simplified model for the function of PP3 in milk, as schematized in Fig. 8. PP3 monomers associate in tetrameric complexes, held together by hydrophobic interactions of the amphipathic α-helices. Milk fatty acids bind to the helices whereby the complex is dissociated into PP3 monomers that can then bind to the fat globules in milk and thereby sterically protect these from lipolysis by endogenous lipases. Furthermore, PP3 monomers are also subject to proteolysis by plasmin, which can lead to the release of the C-terminal peptide, lactophoricin, which can then act as an antibacterial agent in milk or in the digestive tract of the neonate.

Materials and methods

Chemicals (of analytical grade unless otherwise specified) were obtained from Merck (Darmstadt, Germany), Mallinckrodt Baker (Deventeer, The Netherlands) and Sigma (Steinheim, Germany). The Vydac C_4 column was from The Separations Group (Hesperia, CA, USA). The Superdex 200 10/30 GL column was from GE Healthcare (Uppsala, Sweden). DOPC and DOPG were purchased in a powder form from Avanti Polar Lipids (Alabaster, AL, USA). Chloroform (Sigma, St. Louis, MO, USA) was of

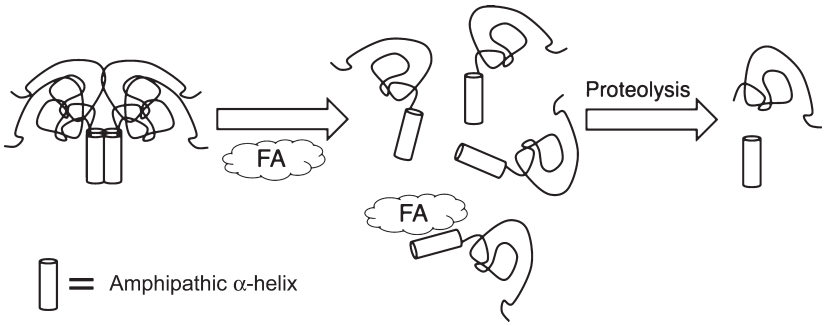

Fig. 8. PP3 tetramers as reservoirs of monomers. Schematic model of how PP3 may associate in tetrameric structures by hydrophobic interaction via the amphipathic helices. The PP3 tetramers may dissociate in the presence of fatty acids (FA) of the milk and protect against lipolysis upon binding the milk fat. Other PP3 monomers could become subject to proteolysis and thereby liberate a peptide, lactophoricin, with antibacterial properties.

≥ 99% purity. DDM was from Calbiochem (Darmstadt, Germany). Oleic acid was from Sigma Aldrich (Stockholm, Sweden). Reagents used for N-terminal amino-acid sequencing were purchased from Applied Biosystems (Foster City, CA, USA). BSA was from Sigma and was of ≥ 98% purity. Polystyrene sulfonate standards were from Postnova analytics GmbH (Landsberg/Lech, Germany).

Purification of PP3

Full-length native PP3 was isolated from bovine milk, as described previously [15]. The identity and purity were verified by N-terminal sequencing analysis and the concentration of PP3 was determined by amino acid analysis. N-terminal sequencing analysis was carried out by automated Edman degradation using an Applied Biosystems Procise protein sequencing system, model 491. A Series 200 (UV/VIS) Detector from PerkinElmer (Waltham, MA, USA) was used for online identification of the phenylthiohydantoin derivatives.

Circular dichroism

CD experiments were performed using a Jasco J-810 spectropolarimeter (Jasco Spectroscopic Co., Hachioji City, Japan) with a Jasco PTC-348W1 temperature control unit. Spectra were recorded from 260 to 190 nm in continuous scanning mode with a response time of 1 s, 0.2-nm steps, a bandwidth of 2 nm and a scan speed of 100 nm·min^{-1}, at 25 °C. Five spectra were accumulated and averaged to increase the signal-to-noise ratio. When lipids were added, the lipid spectrum background was subtracted. Samples were loaded into 0.1-cm path-length quartz cells. PP3 was dissolved in 10 mM Na_2HPO_4 (pH 7.4) containing 1% SDS, 90% TFE or lipid vesicles of either pure DOPC or DOPC/DOPG at a ratio of 80 : 20 (w/w) in a protein:lipid ratio of 1 : 96 (1.27 mM lipid vesicles). The lipid vesicles were prepared from stock solutions of lipids dissolved in chloroform. The lipid solutions were dried under a stream of N_2 and resuspended in 10 mM Na_2HPO_4 (pH 7.4) by vortexing. The resuspended lipids were sonicated by use of a Sonopuls HD2070 homogenizer (Buch & Holm) and a UW2070 converter (both from Bandelin Electronics, Berlin, Germany) for 5 min on ice using 90% pulses at 50% intensity until the solutions were clear. Potential titanium flakes from the probe were removed by centrifugation. All CD wavelength spectra and temperature scans were recorded at protein concentrations between 2.1 and 30 μM using a 1 mm cuvette. For the pH titration, PP3 was dissolved in 10 mM Na_2HPO_4 solutions with pH values between pH 2 and pH 9.2. Temperature scans were recorded at 222 nm, at a scan rate of 1.5 °C per min, in 10 mM Na_2HPO_4 (pH 7.4), with and without 1 mM DDM or 3.5 mM OA. The scan was carried out from 25 to 100 °C, followed by a holding time of 15 min before scanning back to 25 °C. For GdmCl denaturation of PP3, aliquots of GdmCl were added to a fixed concentration of PP3. The mean residue ellipticity (MRE) (θ) was calculated using the equation:

$$[\theta] = \frac{100\theta M_r}{clN_A}, \quad (1)$$

where θ is the CD signal (millidegrees), M_r, is the relative molecular mass, c is the protein concentration (mg·mL^{-1}), l is the path length (cm) and N_A is the number of peptide bonds of the peptide [49].

The thermal stability of PP3 was evaluated by fitting data points to the following equation:

$$Y_{obs} = \frac{\alpha_N + \alpha_U \times exp\left(-\frac{\Delta H_{vh}}{R}\left(\frac{1}{T} - \frac{1}{T_m}\right)\right)}{1 + exp\left(-\frac{\Delta H_{vh}}{R}\left(\frac{1}{T} - \frac{1}{T_m}\right)\right)}, \quad (2)$$

where Y_{obs} is the observed ellipticity, ΔH_{vh} is the van't Hoff enthalpy change, T_m is the temperature where $\Delta G = 0$, and α_N and α_U are the ellipiticities of native and unfolded states, respectively. [50].

GdmCl unfolding data were fitted to the following equation:

$$Y_{obs} = \left(\alpha_N + \alpha_D \times 10^{m_{D-N}([GdmCl]-[GdmCl_{50\%}])}\right) \Big/ \left(1 + 10^{m_{D-N}([GdmCl]-[GdmCl_{50\%}])}\right), \quad (3)$$

where Y_{obs} is the observed signal, α_N and α_D denote the signal at 0 M urea for the native and denatured states, respectively, β_N and β_D are the slopes of the baselines of the native and denatured states and m_{D-N} is the linear dependence of the log of the equilibrium constant of unfolding on [GdmCl], and [$GdmCl_{50\%}$] is the urea concentration where 50% of the protein is denatured [51].

Nonlinear least-squares regression analysis was carried out using KALEIDAGRAPH, version 4.0 (Synergy Software, Reading, PA, USA).

The percentage of α-helicity was estimated using the k2d algorithm on the online server for protein secondary structure analyses from CD spectroscopic data [52,53].

Size-exclusion chromatography

Gel-filtration chromatography was performed on a Superdex 200 10/30 GL gel-filtration column. The column (10 mm × 30 cm) was calibrated in phosphate-buffered saline ($NaCl/P_i$) at a flow rate of 0.8 $mL{\cdot}min^{-1}$. The sample (846 μg of PP3 solubilized in 100 μL of buffer) was applied to the column and absorption was measured at 280 nm. To estimate molecular mass values, the column was calibrated using a low/high-molecular-weight calibration kit (GE Healthcare) containing RNAse A (13 700 Da), carbonic anhydrase (29 000 Da), ovalbumin (44 000 Da), conalbumin (75 000 Da), aldolase (158 000 Da), ferritin (440 000 Da) and blue dextran 2000 (~ 2 000 000 Da).

Asymmetrical flow field-flow fractionation

AF4 is a size-separation technique similar to SEC. However, unlike SEC, separation by the AF4 method has no stationary phase to influence on separation, allowing separation of 'sticky' samples and samples sensitive to shearing forces. When coupled with RI, UV and light-scattering detectors, this allows quantification and size estimates of proteins and protein complexes/aggregates from a lower limit determined by the ultracentrifugation membrane (i.e. down to ~ 1 kDa) and up to well above 10 MDa within the same analysis and sample [54]. AF4 was conducted on a POSTNOVA AF2000 AF4 system (Postnova Analytics GmbH) consisting of two HPLC pumps (tip and focus flows), a syringe pump (cross-flow), the AF4 separation channel, an RI detector (PN3140), a UV/VIS detector (S3240) to monitor the absorbance at 205 nm and a PN3000 MALS to monitor light scatter at seven angles. The trapezoidal shape of the AF4 separation channel was defined by a 350 μm spacer and a 10 kDa MWCO ultrafiltration membrane supplied by the manufacturer. The mobile phase for tip and focus flow was 5 mM Tris/HCl (pH 7.5)/150 mM NaCl.

Twenty microlitres of 7.72 $mg{\cdot}mL^{-1}$ of PP3 dissolved in H_2O was injected and focused inside the AFFF channel using a manual injection port by applying 0.2 $mL{\cdot}min^{-1}$ tip flow, a focus flow of 4.8 and 4.0 $mL{\cdot}min^{-1}$ cross-flow for 3 min, resulting in a detector flow rate of 1 $mL{\cdot}min^{-1}$, which was kept constant throughout the experiment. The elution was initiated by a linear gradient, reducing the focus flow to 0 $mL{\cdot}min^{-1}$ and the tip flow to 5 $mL{\cdot}min^{-1}$ over a 1-min transition period, followed by isocratic elution over 10 min at a cross-flow of 4 $mL{\cdot}min^{-1}$. The cross-flow was then reduced linearly to 2 $mL{\cdot}min^{-1}$ over a 20-min period and further to 0.1 $mL{\cdot}min^{-1}$ over a 10-min period. The cross-flow was then kept at 0.1 $mL{\cdot}min^{-1}$ for 10 min followed by field release at 0 $mL{\cdot}min^{-1}$ for 10 min.

The concentration of the eluting PP3 species was determined by absorbance at 205 nm assuming an ε (205 nm, 0.1%) of 31 and using the RI detector as described: The RI increment factor, dn/dc, of protein conjugates is a function of the dn/dc of the modification and protein, and independent of higher-order structures [55,56], in this case:

$$\left(\frac{dn}{dc}\right)_{PP3} = \frac{M_P}{M_{PP3}}\left(\frac{dn}{dc}\right)_P + \frac{M_P}{M_{PP3}}\left(\frac{dn}{dc}\right)_c \quad (4)$$

where M is the molecular mass (in Da), n is the RI, c is the concentration (in $g{\cdot}mL^{-1}$) and the subscripts p, c and PP3 refer to protein, carbohydrate and PP3 species, respectively.

Because the dn/dc of carbohydrates is essentially invariable [57], a $(dn/dc)_c$ of 0.145 $mL{\cdot}g^{-1}$ for the carbohydrate moieties [56] and a $(dn/dc)_p$ of 0.186 $mL{\cdot}g^{-1}$ for polypeptides (which is essentially independent of amino acid composition [42]) were chosen. The concentration of eluting species was thus determined from the RI detector signal using a calculated $(dn/dc)_{PP3}$ value of 0.181 $mL{\cdot}g^{-1}$.

The molecular mass of the PP3 complex was then determined from MALS data using the Zimm model within the POSTNOVA AF2000 control software version 1.1.027 (Postnova Analytics Inc, Salt Lake City, UT, USA). In brief, MALS, RI or absorbance at 205 nm data were baseline corrected and the Zimm model was applied to estimate the molecular mass of eluting protein species, thus yielding molecular mass estimates for each data point (~ 1 s) by extrapolating scattering data to a zero scattering angle and zero concentration for each data point within the eluting peak.

The absorbance, RI and MALS detectors were calibrated with BSA (66 kDa) and 67 kDa polystyrene sulfonate standards and verified by separation of 5.57 $mg{\cdot}mL^{-1}$ of BSA dissolved in the mobile phase using the same flow programme.

The relative molecular mass of PP3 was obtained from AF4 and SEC by a linear correlation between retention time and molecular mass of the BSA monomer, dimer and trimer peaks, respectively.

Steady-state tyrosine fluorescence

The tertiary structure of PP3 as a function of pH was probed by steady-state tyrosine fluorescence. Fluorescence emission spectra (280–450 nm) were recorded on an LS-55 Luminescence spectrometer (PerkinElmer, Waltham, MA, USA) in 10-mm quartz cells using excitation at 260 nm and 5-nm slit widths. Ten spectra were averaged at a scan speed of 100 nm·min^{-1} at 25 °C. Scans were recorded at a protein concentration of 40 μM in three different buffers: (a) 50 mM glycine (pH 3) containing 150 mM NaCl, (b) 50 mM NaH_2PO_4 (pH 7.4) containing 150 mM NaCl and (c) 50 mM *N*-cyclohexyl-3-aminopropanesulfonic acid (pH 11) containing 150 mM NaCl.

Steady-state fluorescence anisotropy

Samples of 50 μM PP3 and increasing concentrations of GdmCl were excited with vertically polarized light using a PerkinElmer LS55 spectrofluorimeter (PerkinElmer A/S, Hvidovre, Denmark) at room temperature. PP3 was excited at 260 nm and the tyrosine emission was measured at 310 nm using 5-nm slits. The fluorescence anisotropy (r) of intrinsic tyrosine fluorescence was measured in the L-format, according to the following formula [58]:

$$r = \frac{(I_{vv} - GI_{vh})}{(I_{vv} + 2GI_{vh})}, \quad (5)$$

where I_{vv} and I_{vh} are the vertical and horizontal components, respectively, of the fluorescence excited by vertically polarized light, and G is a correction factor characterizing the different sensitivity of the detection system for vertically and horizontally polarized light, as follows:

$$G = \frac{I_{hv}}{2aI_{hh}} \quad (6)$$

where I_{hv} and I_{hh} are the vertical and horizontal components, respectively, of the fluorescence excited by horizontally polarized light.

Anisotropy unfolding data were fitted to Eqn (3) using the same procedure.

Acknowledgements

This work was supported by the Interdisciplinary Nanoscience Center (iNANO) as well as by the Milk Protein Research Consortium. D.E.O. is supported by the Danish Research Foundation (inSPIN). We thank Lise Møller Fogh and Ove Lillelund for excellent technical help.

References

1 Rowland SJ (1937) The soluble fraction of milk. *J Dairy Res* **8**, 6–14.
2 Rowland SJ (1938) The precipitation of the proteins in milk. *J Dairy Res* **9**, 30–41.
3 Paquet D, Nejjar Y & Linden G (1988) Study of a hydrophobic protein fraction isolated from milk proteose-peptone. *J Dairy Sci* **71**, 1464–1471.
4 Andrews AT & Alichanidis E (1983) Proteolysis of caseins and the proteose-peptone fraction of bovine milk. *J Dairy Res* **50**, 275–290.
5 Paquet D (1989) Review: the proteose peptone fraction of milk. *Lait* **69**, 1–21.
6 Kanno C (1989) Purification and separation of multiple forms of lactophorin from bovine milk whey and their immunological and electrophoretical properties. *J Dairy Sci* **72**, 883–891.
7 Kanno C (1989) Characterization of multiple forms of lactophorin isolated from bovine milk whey. *J Dairy Sci* **72**, 1732–1739.
8 Paquet D, Nejjar Y & Alais C (1985) Electrophoretic and chromatographic behavior of the proteose-peptone fraction of cows milk. *Milchwissenschaft* **40**, 200–203.
9 Beg OU, von Bahr-Lindstrom H, Zaidi ZH & Jornvall H (1987) Characterization of a heterogeneous camel milk whey non-casein protein. *FEBS Lett* **216**, 270–274.
10 Cantisani A, Napolitano L, Giuffrida MG & Conti A (1990) Direct identification and characterization of llama (*Lama glama* L.) whey proteins by microsequencing after western blotting. *J Biochem Biophys Methods* **21**, 227–236.
11 Sørensen ES, Rasmussen LK, Moller L & Petersen TE (1997) The localization and multimeric nature of component PP3 in bovine milk: purification and characterization of PP3 from caprine and ovine milks. *J Dairy Sci* **80**, 3176–3181.
12 Lister IM, Rasmussen LK, Johnsen LB, Moller L, Petersen TE & Sørensen ES (1998) The primary structure of caprine PP3: amino acid sequence, phosphorylation, and glycosylation of component PP3 from the proteose-peptone fraction of caprine milk. *J Dairy Sci* **81**, 2111–2115.
13 Rasmussen LK, Johnsen LB, Petersen TE & Sørensen ES (2002) Human GlyCAM-1 mRNA is expressed in the mammary gland as splicing variants and encodes various aberrant truncated proteins. *Immunol Lett* **83**, 73–75.
14 Sørensen ES & Petersen TE (1993) Phosphorylation, glycosylation and amino acid sequence of component PP3 from the proteose peptone fraction of bovine milk. *J Dairy Res* **60**, 535–542.
15 Sørensen ES & Petersen TE (1993) Purification and characterization of three proteins isolated from the proteose peptone fraction of bovine milk. *J Dairy Res* **60**, 189–197.
16 Johnsen LB, Sørensen ES, Petersen TE & Berglund L (1995) Characterization of a bovine mammary gland PP3 cDNA reveals homology with mouse and rat

adhesion molecule GlyCAM-1. *Biochim Biophys Acta* **1260**, 116–118.
17 Groenen MA, Dijkhof RJ & van der Poel JJ (1995) Characterization of a GlyCAM1-like gene (glycosylation-dependent cell adhesion molecule 1) which is highly and specifically expressed in the lactating bovine mammary gland. *Gene* **158**, 189–195.
18 Lasky LA, Singer MS, Dowbenko D, Imai Y, Henzel WJ, Grimley C, Fennie C, Gillett N, Watson SR & Rosen SD (1992) An endothelial ligand for L-selectin is a novel mucin-like molecule. *Cell* **69**, 927–938.
19 Dowbenko D, Watson SR & Lasky LA (1993) Cloning of a rat homologue of mouse GlyCAM 1 reveals conservation of structural domains. *J Biol Chem* **268**, 14399–14403.
20 Dowbenko D, Kikuta A, Fennie C, Gillett N & Lasky LA (1993) Glycosylation-dependent cell adhesion molecule 1 (GlyCAM 1) mucin is expressed by lactating mammary gland epithelial cells and is present in milk. *J Clin Invest* **92**, 952–960.
21 Kanoh N, Dai CF, Tanaka T, Izawa D, Li YF, Kawashima H & Miyasaka M (1999) Constitutive expression of GlyCAM-1 core protein in the rat cochlea. *Cell Adhes Commun* **7**, 259–266.
22 Spencer TE, Bartol FF, Bazer FW, Johnson GA & Joyce MM (1999) Identification and characterization of glycosylation-dependent cell adhesion molecule 1-like protein expression in the ovine uterus. *Biol Reprod* **60**, 241–250.
23 Girardet JM, Coddeville B, Plancke Y, Strecker G, Campagna S, Spik G & Linden G (1995) Structure of glycopeptides isolated from bovine milk component PP3. *Eur J Biochem* **234**, 939–946.
24 Kjeldsen F, Haselmann KF, Budnik BA, Sørensen ES & Zubarev RA (2003) Complete characterization of posttranslational modification sites in the bovine milk protein PP3 by tandem mass spectrometry with electron capture dissociation as the last stage. *Anal Chem* **75**, 2355–2361.
25 Bak M, Sørensen MD, Sørensen ES, Rasmussen LK, Sørensen OW, Petersen TE & Nielsen NC (2000) The structure of the membrane-binding 38 C-terminal residues from bovine PP3 determined by liquid- and solid-state NMR spectroscopy. *Eur J Biochem* **267**, 188–199.
26 Mikkelsen TL, Bakman S, Sørensen ES, Barkholt V & Frokiaer H (2005) Sialic acid-containing milk proteins show differential immunomodulatory activities independent of sialic acid. *J Agric Food Chem* **53**, 7673–7680.
27 Sugahara T, Onda H, Shinohara Y, Horii M, Akiyama K, Nakamoto K & Hara K (2005) Immunostimulation effects of proteose-peptone component 3 fragment on human hybridomas and peripheral blood lymphocytes. *Biochim Biophys Acta* **1725**, 233–240.
28 Grenby TH, Andrews AT, Mistry M & Williams RJ (2001) Dental caries-protective agents in milk and milk products: investigations in vitro. *J Dent* **29**, 83–92.
29 Inagaki M, Nagai S, Yabe T, Nagaoka S, Minamoto N, Takahashi T, Matsuda T, Nakagomi O, Nakagomi T, Ebina T *et al.* (2010) The bovine lactophorin C-terminal fragment and PAS6/7 were both potent in the inhibition of human rotavirus replication in cultured epithelial cells and the prevention of experimental gastroenteritis. *Biosci Biotechnol Biochem* **74**, 1386–1390.
30 Campagna S, Cosette P, Molle G & Gaillard JL (2001) Evidence for membrane affinity of the C-terminal domain of bovine milk PP3 component. *Biochim Biophys Acta* **1513**, 217–222.
31 Campagna S, Mathot AG, Fleury Y, Girardet JM & Gaillard JL (2004) Antibacterial activity of lactophoricin, a synthetic 23-residues peptide derived from the sequence of bovine milk component-3 of proteose peptone. *J Dairy Sci* **87**, 1621–1626.
32 Barzyk W, Campagna S, Wieclaw K, Korchowiec B & Rogalska E (2009) The affinity of two antimicrobial peptides derived from bovine milk proteins for model lipid membranes. *Colloid Surface A* **343**, 104–110.
33 Innocente N, Corradini C, Blecker C & Paqout M (1998) Emulsifying properties of the total fraction and the hydrophobic fraction of the bovine milk proteose-peptones. *Int Dairy J* **8**, 981–985.
34 Courthaudon J-L, Girardet J-M, Chapal C, Lorient D & Linden G (1995) Surface activity and competitive adsorption of milk component 3 and porcine pancretic lipase at the dodecane-water interface. In *Food Macromolecules and Colloids* (Dickinson E & Lorient D, eds.), pp. 58–70. The Royal Society of Chemistry, Cambridge, UK.
35 Ng WC, Brunner JR & Rhee KC (1970) Proteose-peptone fraction of bovine milk: lacteum serum component 3 – a whey glycoprotein. *J Dairy Sci* **53**, 987–996.
36 Sousa A, Passarinha LA, Rodrigues LR, Teixeira JA, Mendonca A & Queiroz JA (2008) Separation of different forms of proteose peptone 3 by hydrophobic interaction chromatography with a dual salt system. *Biomed Chromatogr* **22**, 447–449.
37 Sørensen ES, Rasmussen LK & Petersen TE (1999) Component PP3 from bovine milk is a substrate for transglutaminase. Sequence location of putative cross-linking sites. *J Dairy Res* **66**, 145–150.
38 Ewaschuk JB, Unger S, Harvey S, O'Connor DL & Field CJ (2011) Effect of pasteurization on immune components of milk: implications for feeding preterm infants. *Appl Physiol Nutr Metab* **36**, 175–182.
39 Otzen DE (2011) Protein-surfactant interactions: a tale of many states. *Biochim Biophys Acta* **1814**, 562–591.
40 Otzen DE (2010) Amyloid formation in surfactants and alcohols: membrane mimetics or structural switchers? *Curr Protein Pept Sci* **11**, 355–371.

41 Yohannes G, Wiedmer SK, Elomaa M, Jussila M, Aseyev V & Riekkola ML (2010) Thermal aggregation of bovine serum albumin studied by asymmetrical flow field-flow fractionation. *Anal Chim Acta* **675**, 191–198.
42 Wen J, Arakawa T & Philo JS (1996) Size-exclusion chromatography with on-line light-scattering, absorbance, and refractive index detectors for studying proteins and their interactions. *Anal Biochem* **240**, 155–166.
43 Otzen DE, Sehgal P & Westh P (2009) Alpha-Lactalbumin is unfolded by all classes of surfactants but by different mechanisms. *J Colloid Interface Sci* **329**, 273–283.
44 Sehgal P, Bang Nielsen S, Pedersen S, Wimmer R & Otzen DE (2007) Modulation of cutinase stability and structure by phospholipid detergents. *Biochim Biophys Acta* **1774**, 1544–1554.
45 Månsson HL (2008) Fatty acids in bovine milk fat. *Food & Nutrition Research*, doi:10.3402/fnr.v52i0.1821.
46 Kappeler S, Farh Z & Puhan Z (1999) Alternative splicing og lactophorin mRAN from lactating mammary gland of the camel (*Camelus dromedarius*). *J Dairy Sci* **82**, 2084–2093.
47 Girardet JM, Saulnier F, Gaillard JL, Ramet JP & Humbert G (2000) Camel (*Camelus dromedarius*) milk PP3: evidence for an insertion in the amino-terminal sequence of the camel milk whey protein. *Biochem Cell Biol* **78**, 19–26.
48 Cartier P (1990) Inhibiting and activating effects of skim milks and proteose-peptone fractions on spontaneous lipolysis and purified lipoprotein lipase activity in bovine milk. *J Dairy Sci* **73**, 1173–1177.
49 De Feijter JA, Benjamins J & Veer FA (1978) Ellipsometry as a tool to study the adsorption behavior of synthetic and biopolymers at the air–water interface. *Biopolymers* **17**, 1759–1772.
50 Yadav S & Ahmad F (2000) A new method for the determination of stability parameters of proteins from their heat-induced denaturation curves. *Anal Biochem* **283**, 207–213.
51 Mogensen JE, Ipsen H, Holm J & Otzen DE (2004) Elimination of a misfolded folding intermediate by a single point mutation. *Biochemistry* **43**, 3357–3367.
52 Andrade MA, Chacon P, Merelo JJ & Moran F (1993) Evaluation of secondary structure of proteins from UV circular dichroism spectra using an unsupervised learning neural network. *Protein Eng* **6**, 383–390.
53 Whitmore L & Wallace BA (2008) Protein secondary structure analyses from circular dichroism spectroscopy: methods and reference databases. *Biopolymers* **89**, 392–400.
54 Frauenhofer W & Winter G (2004) The use of asymmetrical flow field-flow fractionation in pharmaceutics and biopharmaceutics. *Eur J Pharm Biopharm* **58**, 369–383.
55 Kunitani M, Dollinger G, Johnson D & Kresin L (1991) On-line characterization of polyethylene glycol-modified proteins. *J Chromatogr* **588**, 125–137.
56 Kendrick BS, Kerwin BA, Chang BS & Philo JS (2001) Online size-exclusion high-performance liquid chromatography light scattering and differential refractometry methods to determine degree of polymer conjugation to proteins and protein-protein or protein-ligand association states. *Anal Biochem* **299**, 136–146.
57 Kunitani M & Kresin L (1993) High-performance liquid chromatographic analysis of carbohydrate mass composition in glycoproteins. *J Chromatogr* **632**, 19–28.
58 Favicchio R, Dragan AI, Kneale GG & Read CM (2009) Fluorescence spectroscopy and anisotropy in the analysis of DNA-protein interactions. *Methods Mol Biol* **543**, 589–611.